Optoacoustic Entanglement in a Continuous Brillouin-Active Solid State System

Changlong Zhu,[1,*] Claudiu Genes,[1,2] and Birgit Stiller[1,2,†]
[1]Max Planck Institute for the Science of Light, Staudtstraße 2, D-91058 Erlangen, Germany
[2]Department of Physics, Friedrich-Alexander-Universität Erlangen-Nürnberg, Staudtstraße 7, D-91058 Erlangen, Germany

(Received 19 January 2024; revised 16 September 2024; accepted 20 September 2024; published 13 November 2024)

Entanglement in hybrid quantum systems comprised of fundamentally different degrees of freedom, such as light and mechanics, is of interest for a wide range of applications in quantum technologies. Here, we propose to engineer bipartite entanglement between traveling acoustic phonons in a Brillouin active solid state system and the accompanying light wave. The effect is achieved by applying optical pump pulses to state-of-the-art waveguides, exciting a Brillouin Stokes process. This pulsed approach, in a system operating in a regime orthogonal to standard optomechanical setups, allows for the generation of entangled photon-phonon pairs, resilient to thermal fluctuations. We propose an experimental platform where readout of the optoacoustics entanglement is done by the simultaneous detection of Stokes and anti-Stokes photons in a two-pump configuration. The proposed mechanism presents an important feature in that it does not require initial preparation of the quantum ground state of the phonon mode.

DOI: 10.1103/PhysRevLett.133.203602

Entanglement between two quantum systems describes a many-body quantum state that is not separable and can exhibit quantum correlations even at arbitrarily large distances [1]. It is therefore a resource not only for a plethora of emerging quantum technologies [2–4] such as quantum cryptography [5,6], quantum teleportation [7,8], and quantum computation [9], but also offers a tool to deeper study and understand the classical-to-quantum boundary [10]. As many experimental endeavors are easier performed under ambient conditions, it is essential to study possibilities of generating entangled quantum states robust to thermal noise even at room temperature. Cavity optomechanics [11], which provides a platform to explore quantum effects via coupling photons and phonons at the macroscale, has been a hot topic of investigations in terms of generation and measurement of entanglement both in theory [12–15] and experiments [16–19].

Continuum optomechanical systems [20,21], such as Brillouin-active optical waveguides [22,23], are a more recent alternative to standard optomechanical cavities, offering a viable platform for the interface between optical photons and continuously accessible groups of acoustic phonons. Such platforms exhibit a powerful performance in quantum information processing with unprecedented acoustic and optical bandwidth compared to cavity optomechanical systems. Especially due to the recent development in nanofabrication, a new breed of chip-based Brillouin-active waveguides with short length (∼cm) have been achieved experimentally [24], which enables coherent information transduction [25], information storage [26,27], and phonon cooling [28,29]. However, the next logical step after the experimental demonstration of Brillouin cooling [29–31] in continuum optomechanics is the observation of quantum optoacoustical entanglement.

In this work, we propose and analyze the feasibility of an experimental scheme (see Fig. 1) which enables the generation of bipartite light-matter entanglement in Brillouin-active waveguides, oriented along the z axis. The mechanism is based on a down-conversion-like process, where pairs of phonons (frequency Ω_{ac}) and Brillouin Stokes scattered photons (frequency ω_s) are generated from the higher energy pump (with $\omega_p = \Omega_{ac} + \omega_s$). As opposed to standard optomechanical systems, the acoustic phonons are highly energetic (in the GHz regime) and mechanical losses (rate Γ) dominate over optical losses (rate γ). This indicates a departure from the standard continuous operation regime and suggests a pulsed operation scheme, thus circumventing the usual prerequisite of initial quantum ground state cooling [16,17]. Based on experimental parameters in accordance with state-of-the-art waveguides [24] utilized for experimental proofs of Brillouin cooling [29–31], we present numerical evidence of optoacoustic entanglement in the pulsed regime achieved without the need of employing nonclassical quantum states of light [32]. At an ambient phonon occupancy n_{th}, for small times $t < 1/(\Gamma n_{th})$ an optimized value for the logarithmic

*Contact author: changlong.zhu@mpl.mpg.de
†Contact author: birgit.stiller@mpl.mpg.de

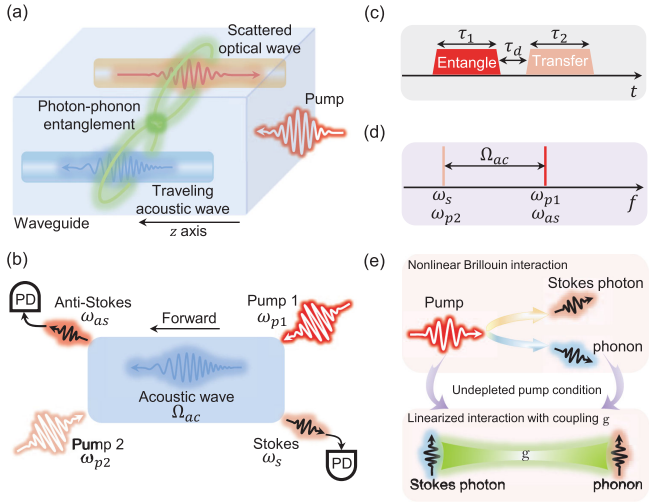

FIG. 1. (a) The Brillouin Stokes scattering implies the down conversion of a pump photon (at ω_p) into a Stokes scattered photon (ω_s) and traveling acoustic phonon (at Ω_{ac}). (b) Protocol for entanglement generation via pump 1 and detection [at photon-diode detectors (PD)] via the simultaneous monitoring of both Stokes and anti-Stokes scattered photons in the presence of pump 2. (c) The timing diagram of the protocol showing the application of an entangling pulse for duration τ_1 followed by the transfer pulse with duration τ_2 after the interval τ_d. (d) The frequency relations between optical and acoustic waves, i.e., $\omega_{p1}-\omega_s=\omega_{as}-\omega_{p2}=\Omega_{ac}$ and $\omega_{as}=\omega_{p1}$. (e) In the linear regime, under the undepleted pump assumption, the nonlinear Brillouin Stokes scattering process can be mapped into a linear Hamiltonian with pump-enhanced coupling strength g.

negativity [33–36] is obtained in a very simple analytical form reading $E_{\mathcal{N}}^{\max}\approx -\ln[1-2g^2/(\Gamma n_{\rm th})^2]$. This entanglement can be detected by homodyne [12] or heterodyne detection [16] of both Stokes photons and anti-Stokes photons produced by a second pump [37] (as illustrated in Fig. 1). More specifically, following the application of a forward-propagating pump with pulse duration τ_1 to stimulate the Brillouin Stokes process, a delayed (delay time τ_d) backward-propagating pulsed pump with duration τ_2 is applied to stimulate the Brillouin anti-Stokes process and thus convert the state of the acoustic phonons to a second optical pulse of the anti-Stokes output wave. Our analytical results and numerical investigations demonstrate that this entanglement generation can be fully optically monitored with reasonable values at temperatures above the restrictive cryogenic regime.

Brillouin Stokes scattering in waveguides—Here we focus on the intramodal Brillouin backward scattering [23], where the Brillouin Stokes and anti-Stokes processes are two independent processes since the two corresponding acoustic waves are counterpropagating [30,38]. Let us first briefly introduce the dynamics of the Brillouin Stokes process under the condition of an undepleted constant cw pump laser (pump 1). In the undepleted pump regime (i.e., undepleted-pump approximation) where the reduction of pump photons can be ignored in comparison with the total pump photon number, the interaction Hamiltonian can be reduced to a linearized optoacoustic parametric down-conversion interaction between scattered photons and acoustic phonons with an effective pump-enhanced coupling strength g [20,28] [illustrated in Fig. 1(e)]. Envelope bosonic operators $a_{\rm s}(z,t)$ and $b_{\rm ac}(z,t)$ at position z along the 1D waveguide can be constructed, corresponding to Stokes and acoustic waves [38–40], i.e., $a_{\rm s}=1/\sqrt{2\pi}\int dk\, a(k,t)e^{-ikz}$ and $b_{\rm ac}=1/\sqrt{2\pi}\int dk\, b(k,t)e^{ikz}$, where $a(k,t)$ and $b(k,t)$ denote annihilation operators for the kth Stokes photon mode and acoustic phonon mode, respectively. This formulation captures the time evolution of the amplitude for each mode. Moving into the momentum space, the dynamics of the linearized Stokes process can be given by [41]

$$\frac{da}{dt}=-\left(\frac{\gamma}{2}+i\Delta_a\right)a-igb^\dagger+\sqrt{\gamma}\xi_a,$$
$$\frac{db}{dt}=-\left(\frac{\Gamma}{2}+i\Delta_b\right)b-iga^\dagger+\sqrt{\Gamma}\xi_b, \tag{1}$$

where γ (Γ) and $\Delta_a=kv_{\rm opt}$ ($\Delta_b=kv_{\rm ac}$) denote the damping rate and wave number-induced frequency shift of the Stokes (acoustic) mode, respectively. Here, $v_{\rm opt}$ ($v_{\rm ac}$) is the group velocity of the Stokes (acoustic) wave. We take the effective coupling strength g real and positive without loss of generality [20]. The quantum noise operators ξ_a and ξ_b are assumed to be zero averaged [11,28,38] and to satisfy the following correlations $\langle\xi_a(t)\xi_a^\dagger(t')\rangle=\delta(t-t')$, $\langle\xi_b^\dagger(t)\xi_b(t')\rangle=n_{\rm th}\delta(t-t')$, and $\langle\xi_b(t)\xi_b^\dagger(t')\rangle=(n_{\rm th}+1)\times\delta(t-t')$. As the frequency of the optical mode is high enough (~193 THz) that the thermal photon occupancy can be neglected even at room temperature, an effective zero temperature bath of the optical mode can be assumed. The thermal phonon occupancy at ambient temperature $T_{\rm m}$ is given by $n_{\rm th}=(e^{\hbar\Omega_{\rm ac}/k_{\rm B}T_{\rm m}}-1)^{-1}$ ($k_{\rm B}$ is the Boltzmann constant).

Optoacoustic entanglement via Brillouin Stokes interaction—In order to quantify entanglement we make use of the logarithmic negativity for continuous variables $E_{\mathcal{N}}$ introduced in Refs. [33–36] and extensively used in Refs. [12,42–46]. To this end, we introduce position and momentum quadratures $x_a=(a+a^\dagger)/\sqrt{2}$, $p_a=i(a^\dagger-a)/\sqrt{2}$, $x_b=(b+b^\dagger)/\sqrt{2}$, and $p_b=i(b^\dagger-b)/\sqrt{2}$. The covariance matrix is then computed $\mathcal{V}_{ij}=[\langle\phi_i(t)\phi_j(t)+\phi_j(t)\phi_i(t)\rangle]/2-\langle\phi_i(t)\rangle\langle\phi_j(t)\rangle$, where the indexes i and j go over the vector $\phi^T(t)=[x_a(t),p_a(t),x_b(t),p_b(t)]$ which is the vector of continuous variables

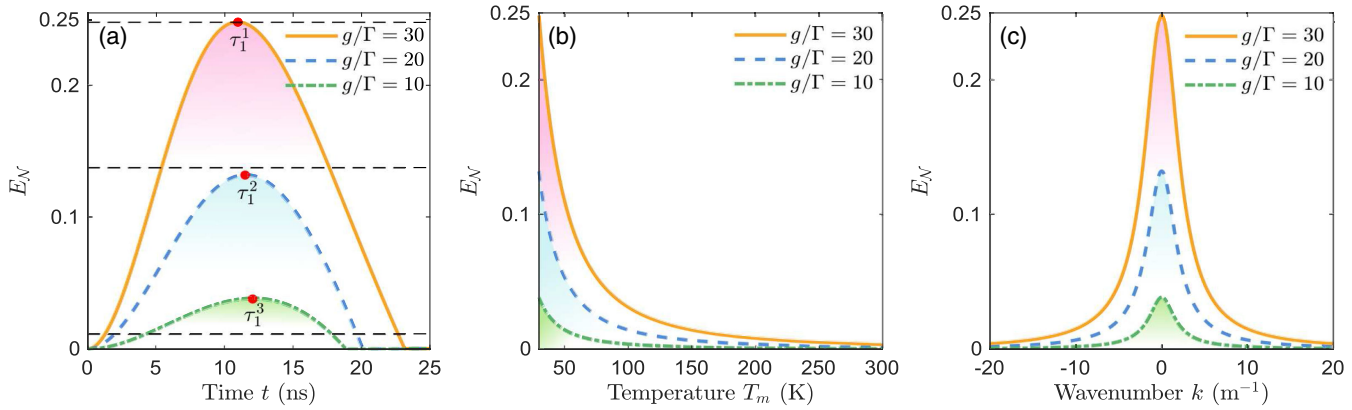

FIG. 2. (a) Time evolution of $E_{\mathcal{N}}$ at $T_{\mathrm{m}} = 30$ K for various ratios g/Γ. The red points denote the optimal time for optimal entanglement and black dashed lines correspond to the maximum value of $E_{\mathcal{N}}$ evaluated by the analytical expression. (b) Variation of $E_{\mathcal{N}}$ versus T_{m} for various ratios g/Γ. (c) Continuum optoacoustic entanglement versus the wave number k in the strong coupling regime at temperature of 30 K.

operators at time t. The symmetric matrix $\mathcal{V}$ can be expressed as the 2×2 block form

$$\mathcal{V} = \begin{bmatrix} A & C \\ C^T & B \end{bmatrix}. \tag{2}$$

From this, one computes $E_{\mathcal{N}} = \max[0, -\ln(2\lambda_-)]$ where λ_- is the minimal symplectic eigenvalue of the covariance matrix $\mathcal{V}$ under a partial transposition [47] and defined as $\lambda_- \equiv 2^{-1/2}\sqrt{\Sigma(\mathcal{V}) - [\Sigma(\mathcal{V})^2 - 4\det\mathcal{V}]^{1/2}}$, with $\Sigma(\mathcal{V}) \equiv \det A + \det B - 2\det C$. As a general criterion for bimodal Gaussian states, entanglement needs the conditions $E_{\mathcal{N}} > 0$, which is equivalent to $\lambda_- < 1/2$. Notice that in the particular case of a two-mode squeezed state, the logarithmic negativity is simply proportional to the squeezing parameter [48,49]. Numerically and analytically one can start with Eqs. (1) to compute the time evolution of the covariance matrix. We perform numerical simulations with experimentally feasible values of system parameters [24,30,50]: $\Gamma/2\pi = 2$ MHz, $\gamma/2\pi = 0.1$ MHz, $\Omega_{\mathrm{ac}}/2\pi = 7.7$ GHz, $c = 3\times10^8$ m/s, $n_{\mathrm{opt}} = 2.4$ (index of refraction), $v_{\mathrm{ac}} = 6000$ m/s, $T_{\mathrm{m}} = 30$ K, and $\Delta_a = 0.2\Gamma$. The results are illustrated in Fig. 2(a) for various ratios of g/Γ in the strong coupling regime and indicate that a given time window is available for efficient optoacoustic entanglement generation. Here the coupling strength in the strong coupling regime is much smaller than the optical and acoustic natural frequencies and the generated Stokes photon number is far smaller than the total pump photon number that guarantees the feasibility of the undepleted-pump approximation. We assume that the wave-number-induced frequency shifts of Stokes and acoustic modes are within the linewidth of the acoustic mode ($\Delta_{a,b} < \Gamma$), where $\Delta_a \gg \Delta_b$ since $v_{\mathrm{opt}} = c/n_{\mathrm{opt}} \gg v_{\mathrm{ac}}$. The Stokes mode is assumed to be initially in the vacuum state while a thermal state with phonon occupation $n_0 = n_{\mathrm{th}} \gg 1$ is assumed for the acoustic mode. Under such conditions, a crude approximation for the minimal symplectic eigenvalue λ_- at a high environment temperature is given by the following expression:

$$\lambda_- \approx \frac{1}{2}\left[1 - 2g^2t^2 + \frac{2}{3}g^2(\Gamma n_{\mathrm{th}})t^3\right]. \tag{3}$$

A better analytical fit to the exact behavior can be obtained, as listed in the Supplemental Material [51], albeit in a quite cumbersome form. However, the simplified expression above suffices to understand the mechanisms leading to the generation and suppression of entanglement. While the initial parametric down-conversion interaction can lead to the generation of entanglement by reducing the symplectic eigenvalue below $1/2$, at a rate indicated by g, the environmental induced decoherence rate $A_{\mathrm{heat}} = \Gamma n_{\mathrm{th}}$ acts in the opposite fashion. The pulse duration that leads to optimal entanglement is found to be on the order of A_{heat}^{-1} and the maximally achievable value of the logarithmic negativity can be estimated by

$$E_{\mathcal{N}}^{\max} \approx -\ln\left[1 - 2\left(\frac{g}{A_{\mathrm{heat}}}\right)^2\right]. \tag{4}$$

The result shows that a necessary condition for such a pulsed scheme to generate considerable entanglement is that the coupling strength overcomes the thermal reheating rate: this is validated by numerical simulations shown in Fig. 2(a). The robustness of such optoacoustic entanglement with respect to environment temperature is presented in Fig. 2(b), showing that high values of optoacoustic entanglement, comparable to other recent results [52–54], can be achieved at a temperature of tens of Kelvins. For example, using the setup of Ref. [30], for a waveguide with the length $L = 0.5$ m and Brillouin gain $G_B = 300\ \mathrm{m^{-1}\,W^{-1}}$, it should be possible to create entangled

photon-phonon pairs with $E_{\mathcal{N}} = 0.3$ at a temperature of 30K by utilizing a pulsed pump with duration of 11 ns and peak power of 0.5 W.

It should be noted that we only consider the case with a specific wave number k in the above discussion. However, the optical and acoustic waves provide groups of photons and phonons in a continuous optomechanical system [37–41]. Therefore, the system has the capability of producing optoacoustic entanglement over a wide bandwidth of Stokes photons and acoustic phonons. This is illustrated in Fig. 2(c) which shows that the negativity $E_{\mathcal{N}}$ can achieve considerable values over a large interval of wave numbers k, indicating high degree of entanglement over accessible groups of photons and phonons in Brillouin-active waveguides at high environmental temperatures, which is a crucial aspect for a broad range of applications, such as quantum computing [55], quantum communication [56], and sensing [57].

Optical readout of entanglement—Although the detection of the optical Stokes field can be directly performed by an optical heterodyne [15,58] or homodyne measurements [12], direct access to the quantum state of the acoustic field is not easily experimentally achievable. This difficulty can be overcome by transducing the mechanical quantum state into the quantum state of an auxiliary optical mode, followed by standard homodyne detection on such mode. To this end, we propose to employ an additional backward-propagating pump, delayed by time τ_d, as shown in Figs. 1(b) and 1(c). This maps the phonon state into anti-Stokes photons through Brillouin anti-Stokes scattering [37]. In the undepleted pump regime, this process can be treated as a beam-splitter interaction. Such an interaction would lead to a full quantum state swap between the two modes; the additional presence of decoherence mechanisms simply degrades the fidelity of the swapping process thus requiring finite and quick swap pulses. In terms of quantum Langevin equations this can be cast as

$$\begin{aligned}\frac{d\tilde{a}}{dt} &= -\left(\frac{\gamma}{2} + i\Delta_{\tilde{a}}\right)\tilde{a} - i\tilde{g}b + \sqrt{\gamma}\xi_{\tilde{a}},\\ \frac{db}{dt} &= -\left(\frac{\Gamma}{2} + i\Delta_b\right)b - i\tilde{g}\,\tilde{a} + \sqrt{\Gamma}\xi_b,\end{aligned} \tag{5}$$

where $\tilde{a}$ is the bosonic operator referring at the anti-Stokes mode and we assumed that its loss rate is the same as the one of the Stokes mode γ. Notice that $\tilde{g}$ denotes the effective coupling strength between the anti-Stokes photons and acoustic phonons. The swapping dynamics can be simply understood from the analytical expression of the number of successfully transferred anti-Stokes quanta. In the strong coupling regime, to a good approximaton, this is given by $e^{-(\gamma+\Gamma)t/2}(1-\cos 2\tilde{g}t)n_b/2$, where $t > 0$ is the time counter during the readout pulse while n_b corresponds to the phonon number at the beginning of swapping time $\tau_1 + \tau_d$. The result shows that an optimal swap is realized

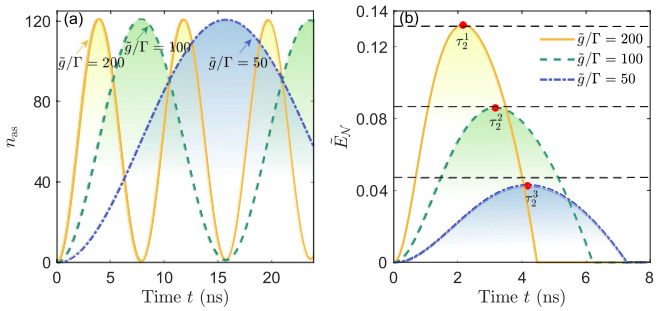

FIG. 3. (a) Time evolution of the anti-Stokes photon occupation $n_{\rm as}(t)$ in the strong coupling regime at 30K for various ratios $\tilde{g}/\Gamma$ during the optical readout process ($t \in [\tau_1 + \tau_d, \tau_1 + \tau_d + \tau_2]$). (b) Corresponding bipartite entanglement between optical modes, where red points denote the optimal time for optimal entanglement and black dashed lines correspond to the maximum value of $\tilde{E}_{\mathcal{N}}$ evaluated by the fully analytical expression. The coupling strength in the entanglement process is fixed to $g/\Gamma = 30$.

at $t = \pi/(2\tilde{g})$ and affected by the exponential process stemming from optical and phonon decoherence. The time evolution of $n_{\rm as}(t)$ for various coupling strengths $\tilde{g}$ is illustrated in Fig. 3(a).

Let us now move onto the characterization of the observable entanglement between the Stokes and anti-Stokes modes. To this end we solve Eqs. (5) both analytically and numerically for the all optical logarithmic negativity $\tilde{E}_{\mathcal{N}}$. After some approximations, a simplified expression of the minimal symplectic eigenvalue $\tilde{\lambda}_-$ can be casted in the following form:

$$\tilde{\lambda}_- \approx \frac{1}{2}\left[1 - \eta^2 t^2 + \frac{2}{3}\tilde{g}^2(\Gamma n_{\rm th})t^3\right], \tag{6}$$

which resembles the solution obtained for the optoacoustic entanglement in Eq. (3) up to third order in t with an entanglement generation coefficient η and the decoherence term identical as previously derived. The analytical expression for the entanglement readout rate is

$$\eta^2 = \frac{\tilde{g}^2(\mathcal{C}_{ns}^2 - 4n_b n_s)}{1 + 2n_s}, \tag{7}$$

with notations n_s and $\mathcal{C}_{ns}$ standing for the Stokes photon occupancy and cross-correlation between Stokes photons and acoustic phonons at time $\tau_1 + \tau_d$ (for more details see Supplemental Material [51]). The solution is remarkably similar to the one in Eq. (3) with the striking difference that the entanglement readout rate depends on the produced entanglement in the write-in part. This can be immediately observed in the expression $\mathcal{C}_{ns}^2 - 4n_b n_s$ indicating that cross-correlations are needed in order to swap entanglement. As a simple intuitive check, higher temperatures automatically reduce the swapping rate, as the product $n_b n_s$

increases, up to the point η becomes negative and entanglement readout is no longer possible.

Numerical simulations are illustrated in Fig. 3(b) for various ratios of $\tilde{g}/\Gamma$, where the red points correspond to the optimal pulse duration τ_2 for various $\tilde{g}$, respectively. At an environmental temperature around 30K, the thermal noise is considerable and needs a fast readout time as shown in Fig. 3(b). Realistically, this can be obtained in a pulsed scheme where the entangling pump duration of 11 ns and peak power of 0.5 W is followed by a counter-propagating pump with duration of 3 ns and peak power of 5 W after 0.1 ns delay. We assume a waveguide with the length $L = 0.5$ m and Brillouin gain $G_B = 300\ \mathrm{m^{-1}\,W^{-1}}$ as achieved in Ref. [30]. For an environmental temperature of 30K, the optoacoustic entanglement of peak value $E_{\mathcal{N}} = 0.3$ will be transduced in an photon-photon entanglement of peak value $\tilde{E}_{\mathcal{N}} = 0.1$.

The generation and synchronization of the pump pulses can be implemented via high-extension ratio modulators as in Refs. [26,27]. The detection of the entangled states is feasible with double homodyne detection for measuring the X and P variables. Accurate characterization of the electronic noise of the electronic amplifiers and detectors will be necessary as well as proper analysis of the statistics. However, these techniques are quite far developed for quantum communication systems [59]. Another experimental challenge will be the separation of the pump pulses and the entangled signals which can likely be addressed by a combination of using different polarizations for the two pumps as well as time gating of the pump and signal pulses.

Conclusions and outlook—We have shown that optoacoustic entanglement in continuous media, over groups of photons and phonon modes can be achieved through the nonlinear optical process of Brillouin scattering. As opposed to standard optomechanics, characterized by extremely high mechanical Q resonators and by operation under steady state conditions, the large mechanical loss characterizing such setups imply operation in the pulsed regime. This presents itself as an advantage, as the possibility of reaching strong phonon-photon coupling allows for the quick generation of entanglement, even in the presence of strong reheating rates. Our estimates show that, utilizing state-of-the-art waveguides where continuous optomechanical cooling has been proved [30], the generated optoacoustic entanglement can survive in thermal environments far from the exclusive cryogenic requirements. Moreover, quantum ground state cooling of the acoustic mode in this case is not a prerequisite. The generated bimodal optoacoustic entanglement can be read out by optical detection means, namely, by homodyne monitoring of both Stokes and anti-Stokes photons stemming from two different pumps which share the same propagating acoustic mode. The fact that the system operates over a large bandwidth of both optical and acoustic modes brings a new prospect of entanglement with continuum modes with great potential for applications in quantum computation [55], quantum storage [56], quantum metrology [57], quantum teleportation [60], entanglement-assisted quantum communication [61], and the exploration of the boundary between classical and quantum worlds [62].

Acknowledgments—This work is supported by the Max-Planck-Society through the independent Max Planck Research Groups Scheme and the Deutsche Forschungsgemeinschaft (DFG, German Research Foundation)—Project-ID 429529648—TRR 306 QuCoLiMa ("Quantum Cooperativity of Light and Matter").

[1] A. Einstein, B. Podolsky, and N. Rosen, Can quantum-mechanical description of physical reality be considered complete?, Phys. Rev. **47**, 777 (1935).
[2] D. Bouwmeester, A. Ekert, and A. Zeilinger, *The Physics of Quantum Information* (Springer, Berlin, 2000).
[3] S. L. Braunstein and P. Van Loock, Quantum information with continuous variables, Rev. Mod. Phys. **77**, 513 (2005).
[4] R. Horodecki, P. Horodecki, M. Horodecki, and K. Horodecki, Quantum entanglement, Rev. Mod. Phys. **81**, 865 (2009).
[5] A. K. Ekert, Quantum cryptography based on Bell's theorem, Phys. Rev. Lett. **67**, 661 (1991).
[6] T. Jennewein, C. Simon, G. Weihs, H. Weinfurter, and A. Zeilinger, Quantum cryptography with entangled photons, Phys. Rev. Lett. **84**, 4729 (2000).
[7] C. H. Bennett, G. Grassard, C. Crepeau, R. Jozsa, A. Peres, and W. K. Wootters, Teleporting an unknown quantum state via dual classical and Einstein-Podolsky-Rosen channels, Phys. Rev. Lett. **70**, 1895 (1993).
[8] S. G. Hofer, W. Wieczorek, M. Aspelmeyer, and K. Hammerer, Quantum entanglement and teleportation in pulsed cavity optomechanics, Phys. Rev. A **84**, 052327 (2011).
[9] D. Gottesman and I. L. Chuang, Demonstrating the viability of universal quantum computation using teleportation and single-qubit operations, Nature (London) **402**, 390 (1999).
[10] A. J. Leggett, Testing the limits of quantum mechanics: Motivation, state of play, prospects, J. Phys. Condens. Matter **14**, R415 (2002).
[11] M. Aspelmeyer, T. J. Kippenberg, and F. Marquardt, Cavity optomechanics, Rev. Mod. Phys. **86**, 1391 (2014).
[12] D. Vitali, S. Gigan, A. Ferreira, H. R. Böhm, P. Tombesi, A. Guerreiro, V. Vedral, A. Zeilinger, and M. Aspelmeyer, Optomechanical entanglement between a movable mirror and a cavity field, Phys. Rev. Lett. **98**, 030405 (2007).
[13] M. Paternostro, D. Vitali, S. Gigan, M. S. Kim, C. Brukner, J. Eisert, and M. Aspelmeyer, Creating and probing multipartite macroscopic entanglement with light, Phys. Rev. Lett. **99**, 250401 (2007).
[14] C. Genes, A. Mari, P. Tombesi, and D. Vitali, Robust entanglement of a micromechanical resonator with output optical fields, Phys. Rev. A **78**, 032316 (2008).

[15] A. K. Sarma, S. Chakraborty, and S. Kalita, Continuous variable quantum entanglement in optomechanical systems: A short review, AVS Quant. Sci. **3**, 015901 (2021).
[16] T. A. Palomaki, J. D. Teufel, R. W. Simmonds, and K. W. Lehnert, Entangling mechanical motion with microwave fields, Science **342**, 710 (2013).
[17] C. F. Ockeloen-Korppi, E. Damskägg, J.-M. Pirkkalainen, M. Asjad, A. A. Clerk, F. Massel, M. J. Woolley, and M. A. Sillanpää, Stabilized entanglement of massive mechanical oscillators, Nature (London) **556**, 478 (2018).
[18] I. Marinkovic, A. Wallucks, R. Riedinger, S. Hong, M. Aspelmeyer, and S. Gröblacher, Optomechanical Bell test, Phys. Rev. Lett. **121**, 220404 (2018).
[19] S. Barzanjeh, E. S. Redchenko, M. Peruzzo, M. Wulf. D. P. Lewis, G. Arnold, and J. M. Fink, Stationary entangled radiation from micromechanical motion, Nature (London) **570**, 480 (2019).
[20] R. Van Laer, R. Baets, and D. Van Thourhout, Unifying Brillouin scattering and cavity optomechanics, Phys. Rev. A **93**, 053828 (2016).
[21] P. Rakich and F. Marquardt, Quantum theory of continuum optomechanics, New J. Phys. **20**, 045005 (2018).
[22] C. Wolff, M. J. Steel, B. J. Eggleton, and C. G. Poulton, Stimulated Brillouin scattering in integrated photonic waveguides: Forces, scattering mechanisms, and coupled-mode analysis, Phys. Rev. A **92**, 013836 (2015).
[23] C. Wolff, M. J. A. Smith, B. Stiller, and C. G. Poulton, Brillouin scattering—Theory and experiment: Tutorial, J. Opt. Soc. Am. B **38**, 1243 (2021).
[24] B. J. Eggleton, C. G. Poulton, P. T. Rakich, M. J. Steel, and G. Bahl, Brillouin integrated photonics, Nat. Photonics **13**, 664 (2019).
[25] H. Shin, J. A. Cox, R. Jarecki, A. Starbuck, Z. Wang, and P. T. Rakich, Control of coherent information via on-chip photonic-phononic emitter-receivers, Nat. Commun. **6**, 6427 (2015).
[26] M. Merklein, B. Stiller, K. Vu, S. J. Madden, and B. J. Eggleton, A chip-integrated coherent photonic-phononic memory, Nat. Commun. **8**, 574 (2017).
[27] B. Stiller, M. Merklein, C. Wolff, K. Vu, P Ma, S. J. Madden, and B. J. Eggleton, Coherently refreshing hypersonic phonons for light storage, Optica **7**, 492 (2020).
[28] Y.-C. Chen, S. Kim, and G. Bahl, Brillouin cooling in a linear waveguide, New J. Phys. **18**, 115004 (2016).
[29] N. T. Otterstrom, R. O. Behunin, E. A. Kittlaus, and P. T. Rakich, Optomechanical cooling in a continuous system, Phys. Rev. X **8**, 041034 (2018).
[30] L. B. Martinez, P. Wiedemann, C. L. Zhu, A. Geilen, and B. Stiller, Optoacoustic cooling of traveling hypersound waves, Phys. Rev. Lett. **132**, 023603 (2024).
[31] J. N. Johnson, D. R. Haverkamp, Y.-H. Ou, K. Kieu, N. T. Otterstrom, P. T. Rakich, and R. O. Behunin, Laser cooling of traveling wave phonons in an optical fiber, Phys. Rev. Appl. **20**, 034047 (2023).
[32] P. Sekatski, M. Aspelmeyer, and N. Sangouard, Macroscopic optomechanical from displaced single-photon entanglement, Phys. Rev. Lett. **112**, 080502 (2014).
[33] K. Życzkowski, P. Horodecki, A. Sanpera, and M. Lewenstein, Volume of the set of separable states, Phys. Rev. A **58**, 883 (1998).
[34] G. Vidal and R. F. Werner, Computable measure of entanglement, Phys. Rev. A **65**, 032314 (2002).
[35] M. B. Plenio, The logarithmic negativity: A full entanglement monotone that is not convex, Phys. Rev. Lett. **95**, 090503 (2005).
[36] G. Adesso, A. Serafini, and F. Illuminati, Extremal entanglement and mixedness in continuous variable systems, Phys. Rev. A **70**, 022318 (2004).
[37] J. Y. Zhang, C. L. Zhu, C. Wolff, and B. Stiller, Quantum coherent control in pulsed waveguide optomechanics, Phys. Rev. Res. **5**, 013010 (2023).
[38] P. Kharel, R. O. Behunin, W. H. Renninger, and P. T. Rakich, Noise and dynamics in forward Brillouin scattering, Phys. Rev. A **93**, 063806 (2016).
[39] J. E. Sipe and M. J. Steel, A Hamiltonian treatment of stimulated Brillouin scattering in nanoscale integrated waveguides, New J. Phys. **18**, 045004 (2016).
[40] H. Zoubi and K. Hammerer, Optomechanical multimode Hamiltonian for nanophotonic waveguides, Phys. Rev. A **94**, 053827 (2016).
[41] C. L. Zhu and B. Stiller, Dynamic Brillouin cooling for continuous optomechanical systems, Mater. Quant. Technol. **3**, 015003 (2023).
[42] B. Rogers, M. Paternostro, G. M. Palma, and G. De Chiara, Entanglement control in hybrid optomechanical systems, Phys. Rev. A **86**, 042323 (2012).
[43] Y. D. Wang and A. A. Clerk, Reservoir-engineered entanglement in optomechanical systems, Phys. Rev. Lett. **110**, 253601 (2013).
[44] L. Tian, Robust photon entanglement via quantum interference in optomechanical interfaces, Phys. Rev. Lett. **110**, 233602 (2013).
[45] S. S. Zheng, F. X. Sun, Y. j. Lai, Q. H. Gong, and Q. Y. He, Manipulation and enhancement of asymmetric steering via interference effects induced by closed-loop coupling, Phys. Rev. A **99**, 022335 (2019).
[46] F. X. Sun, S. S. Zheng, Y. Xiao, Q. H. Gong, Q. Y. He, and K. Xia, Remote generation of magnon Schrödinger cat state via magnon-photon entanglement, Phys. Rev. Lett. **127**, 087203 (2021).
[47] S. Pirandola, A. Serafini, and S. Lloyd, Correlation matrices of two-mode bosonic systems, Phys. Rev. A **79**, 052327 (2009).
[48] S. Zippilli and F. Illuminati, Non-Markovian dynamics and steady-state entanglement of cavity arrays in finite-bandwidth squeezed reservoirs, Phys. Rev. A **89**, 033803 (2014).
[49] S. Zippilli, G. Di Giuseppe, and D. Vitali, Entanglement and squeezing of continuous-wave stationary light, New J. Phys. **17**, 043025 (2015).
[50] M. Merklein, A. Gasas-Bedoya, D. Marpaung, T. F. S. Büttner, M. Pagani, B. Morrison, I. V. Kabakova, and B. J. Eggleton, Stimulated Brillouin scattering in photonic integrated circuits: Novel applications and devices, IEEE J. Sel. Top. Quant. Eletron. **22**, 336 (2016).
[51] See Supplemental Material at http://link.aps.org/supplemental/10.1103/PhysRevLett.133.203602, which includes Refs. [20, 33–34, 36, 38–40, 47], for additional information about the detailed derivation and discussion of the dynamics of the system, the entanglement generation, and measurement.

[52] M. Yu, H. Shen, and J. Li, Magnetostrictively induced stationary entanglement between two microwave fields, Phys. Rev. Lett. **124**, 213604 (2020).
[53] Y. F. Jiao, S. D. Zhang, Y. L. Zhang, A. Miranowicz, L. M. Kuang, and H. Jing, Nonreciprocal optomechanical entanglement against backscattering losses, Phys. Rev. Lett. **125**, 143605 (2020).
[54] D. G. Lai, J. Q. Liao, A. Miranowicz, and F. Nori, Noise-tolerant optomechanical entanglement via synthetic magnetism, Phys. Rev. Lett. **129**, 063602 (2022).
[55] U. L. Andersen, J. S. Neergaard-Nielsen, P. van Loock, and A. Furusawa, Hybrid discrete- and continuous-variable quantum information, Nat. Phys. **11**, 713 (2015).
[56] E. Saglamyurek, N. Sinclair, J. Jin, J. A. Slater, D. Oblak, F. Bussières, M. George, R. Sohler, and W. Tittel, Broadband waveguide quantum memory for entangled photons, Nature (London) **469**, 512 (2011).
[57] Y. Xia, A. R. Agrawal, C. M. Pluchar, A. J. Brady, Z. Liu, Q. Zhuang, D. J. Wilson, and Z. Zhang, Entanglement-enhanced optomechanical sensing, Nat. Photonics **17**, 470 (2023).
[58] R. Sahu, L. Qiu, W. Hease, G. Arnold, Y. Minoguchi, P. Rabl, and J. M. Fink, Entangling microwaves with optical light, Science **380**, 718 (2023).
[59] S. Richter, M. Thornton, I. Khan, H. Scott, K. Jaksch, U. Vogl, B. Stiller, G. Leuchs, C. Marquardt, and N. Korolkova, Agile and versatile quantum communication: Signatures and secrets, Phys. Rev. X **11**, 011038 (2021).
[60] S. Barzanjeh, M. Abdi, G. J. Milburn, P. Tombesi, and D. Vitali, Reversible optical-to-microwave quantum interface, Phys. Rev. Lett. **109**, 130503 (2012).
[61] A. Piveteau, J. Pauwels, E. Håkansson, S. Muhammad, M. Bourennane, and A. Tavakoli, Entanglement-assisted quantum communication with simple measurement, Nat. Commun. **13**, 7878 (2022).
[62] W. H. Zurek, Decoherence, einselection, and the quantum origions of the classical, Rev. Mod. Phys. **75**, 715 (2003).